Angewandte Chemie International Edition

Angewandte International Edition Chemie

How to cite: *Angew. Chem. Int. Ed.* **2026**, e23506
doi.org/10.1002/anie.202523506

MINIREVIEW OPEN ACCESS

Ethane Chlorination Toward Vinyl Chloride Synthesis: Mechanistic and Catalytic Perspectives

Xia Wu[1,2] | Guodong Huo[1] | Haifeng Qi[3] | Qinggang Liu[1,3] | Nicholas F. Dummer[3] | Graham J. Hutchings[3] | Yanqiang Huang[1]

[1]State Key Laboratory of Catalysis, Dalian Institute of Chemical Physics, Chinese Academy of Sciences, Dalian, China | [2]Chemical Engineering and Resource Utilization, Northeast Forestry University, Harbin, China | [3]Max Planck-Cardiff Centre on the Fundamentals of Heterogeneous Catalysis FUNCAT, Cardiff Catalysis Institute, Translational Research Hub, Cardiff University, Cardiff, UK

Correspondence: Qinggang Liu (liuqg@dicp.ac.cn) | Nicholas F. Dummer (DummerNF@cardiff.ac.uk) | Graham J. Hutchings (Hutch@cardiff.ac.uk)

Received: 26 October 2025 | **Revised:** 17 December 2025 | **Accepted:** 26 January 2026

Keywords: ethane chlorination | heterogeneous catalysis | radical chemistry | rare-earth oxychlorides | vinyl chloride monomer

ABSTRACT

Ethane chlorination has emerged as a promising alternative to conventional ethylene- and acetylene-based routes for the production of vinyl chloride monomer (VCM). Unlike conventional catalytic processes, this approach relies on chlorine radical-mediated activation to convert ethane into 1,2-dichloroethane, followed by thermal cracking to VCM. However, this route remains in its early stages, hindered by the complexity of gas-phase radical chemistry and catalyst deactivation under chlorination conditions. This review provides a critical assessment of the mechanistic foundations of ethane chlorination, highlighting the interplay between radical-mediated and surface-catalyzed pathways. Particular attention is given to advances in rare-earth oxychloride catalysts, which have shown the ability to stabilize key intermediates. We also discuss major deactivation mechanisms, including phase transformation and surface hydroxylation, that limit catalyst lifetime. Furthermore, we highlight the feasibility of ethane chlorination as a low-carbon VCM production route under future decarbonized energy scenarios. Finally, key directions in catalyst design, mechanistic understanding, and process integration are outlined to advance ethane chlorination from laboratory-scale innovation to industrial reality.

1 | Introduction

Polyvinyl chloride (PVC), the third most produced synthetic polymer, plays a crucial role in applications ranging from construction materials to medical devices [1–5]. Its precursor, vinyl chloride monomer (VCM), is currently synthesized through the acetylene (C_2H_2) hydrochlorination and the ethylene (C_2H_4) balanced process (Figure 1a,b, respectively) [6–11]. While the former still relies on mercury-containing catalysts with severe environmental and health consequences [12, 13], the latter depends on oil-derived C_2H_4 and entails a multistep process involving chlorination, oxychlorination, and thermal cracking [14–22]. Both traditional routes are energy- and carbon-intensive, with the C_2H_4-based pathway emitting ~2 kg CO_2-eq kg^{-1} of VCM [23]. Coupled with rising oil prices and tightening regulations on carbon and mercury emissions, these processes have become increasingly unsustainable [24, 25].

Accordingly, increasing attention has turned to the direct chlorination of light alkanes as an alternative strategy for VCM production. Building on insights gained from methane (CH_4) chlorination, where selective C–Cl bond formation from Cl_2 has

Xia Wu and Guodong Huo contributed equally to this work.

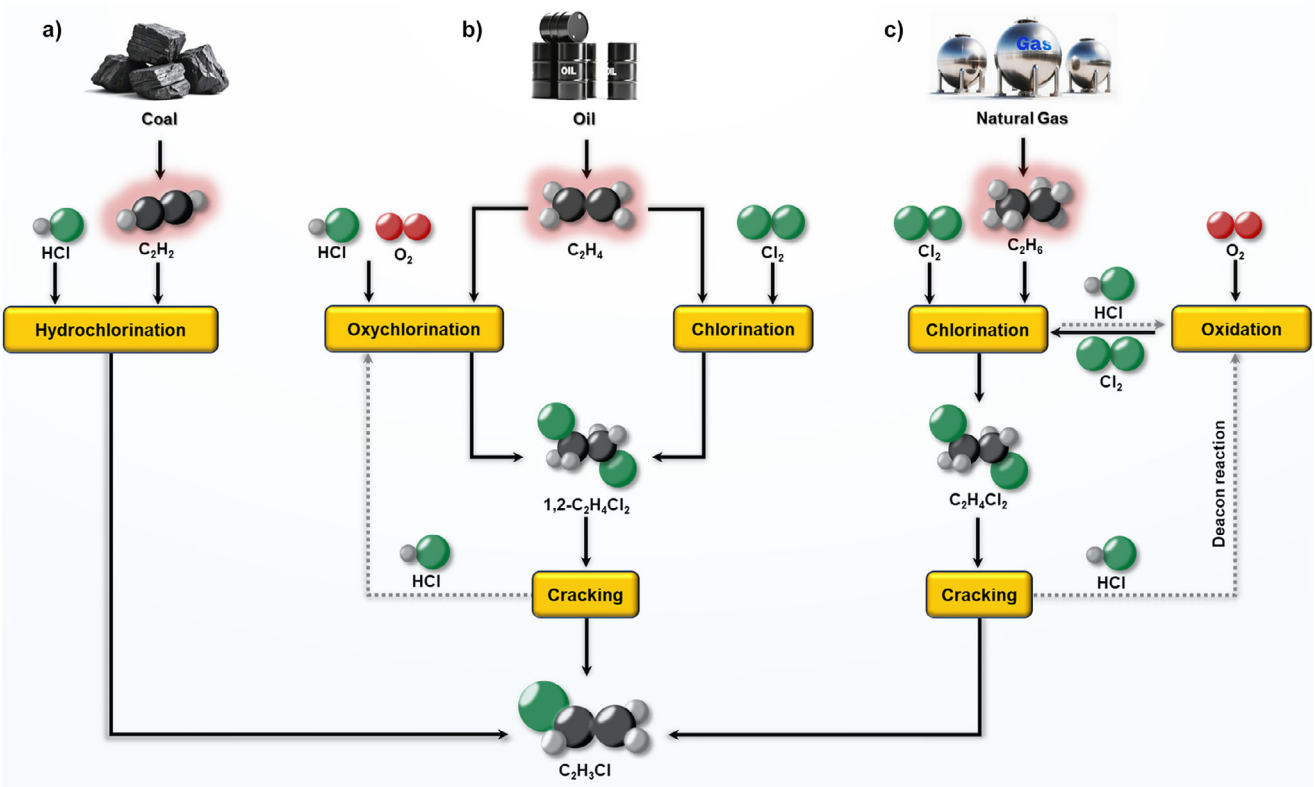

FIGURE 1 | Schematic illustration of VCM synthesis via C_2H_2 hydrochlorination (a), the C_2H_4-based balanced process (b), and C_2H_6 chlorination (c).

been demonstrated under catalytic conditions [26, 27], ethane (C_2H_6) has emerged as a particularly attractive feedstock [28–33]. Chlorination of C_2H_6 to 1,2-dichloroethane ($1,2\text{-}C_2H_4Cl_2$), followed by its established thermal cracking to VCM, offers a promising route that bypasses the need for C_2H_4 or C_2H_2 (Figure 1c) [34]. Notably, as the cracking step is already a commercially proven and well-optimized technology, research efforts can focus primarily on improving the selective chlorination of C_2H_6 rather than reinventing the entire VCM production chain. Compared to C_2H_4-based routes, C_2H_6 chlorination has been projected to reduce production costs by over 30% under current conditions [23].

Despite its advantages, the industrial implementation of C_2H_6 chlorination remains challenging due to the complex nature of its reaction chemistry. The conversion of C_2H_6 to $1,2\text{-}C_2H_4Cl_2$ is predominantly governed by radical mechanisms initiated by chlorine radicals (•Cl). Hydrogen atoms are abstracted from C_2H_6 by •Cl, generating ethyl radicals that further react with •Cl to form chloroethane (C_2H_5Cl) and ultimately dichlorinated products [35]. While efficient at initiating C–H activation, •Cl radicals are highly unselective, often promoting over-chlorination and dehydrochlorination side reactions. As a result, maintaining product selectivity becomes increasingly difficult at higher C_2H_6 conversions.

Heterogeneous catalysts—particularly rare-earth oxychlorides like LaOCl and EuOCl—have been explored to modulate radical reactivity and improve selectivity [36, 37]. These catalysts offer sites for •Cl stabilization and facilitate regioselective hydrogen abstraction. However, under Cl_2-rich conditions, LaOCl is prone to irreversible transformation into $LaCl_3$, a phase with significantly diminished catalytic activity. Additional challenges such as surface hydroxylation and sintering further degrade catalyst performance and shift product distribution toward undesired species [35]. Adding to the complexity is the multifaceted nature of the reaction system, where gas-phase radical chemistry and surface-mediated catalysis coexist and interact dynamically. This duality makes it difficult to decouple kinetic effects, complicates reactor design, and limits the effectiveness of conventional catalytic control strategies. Achieving industrially relevant performance will require a new generation of materials informed by a fundamental understanding of radical–surface interactions.

In light of these considerations, this review aims to provide a comprehensive and critical assessment of C_2H_6 chlorination as a platform for low-carbon VCM production. We begin by outlining the mechanistic foundations of gas-phase •Cl-mediated C_2H_6 chlorination, followed by a discussion of recent advances in catalyst design, structure–function relationships, and deactivation mechanisms. We then evaluate the techno-economic and environmental performance of C_2H_6-based routes in comparison to conventional technologies. Finally, we highlight key challenges and research priorities that need to be addressed to enable the industrial realization of this emerging process. By providing a unified view of reaction mechanisms and catalyst design principles, this work offers a comprehensive foundation for the development of next-generation chlorination technologies centered on natural gas feedstocks.

2 | Ethane Chlorination Chemistry

2.1 | Reaction Thermodynamics of C_2H_6 Chlorination

The chlorination of C_2H_6 to 1,2-$C_2H_4Cl_2$ involves two consecutive radical-mediated steps, with hydrogen chloride (HCl) as a co-product. The balanced overall reactions are:

$$C_2H_6 + Cl_2 \rightarrow C_2H_5Cl + HCl, \Delta H^{o}_{303K} = -142 \text{ kJ mol}^{-1}$$

$$C_2H_5Cl + Cl_2 \rightarrow 1,2 - C_2H_4Cl_2 + HCl, \Delta H^{o}_{303K} = -131 \text{ kJ mol}^{-1}$$

Alternatively, the net reaction can be summarized as:

$$C_2H_6 + 2Cl_2 \rightarrow 1,2 - C_2H_4Cl_2 + 2HCl, \Delta H^{o}_{303K} = -273 \text{ kJ mol}^{-1}$$

In conventional C_2H_4-based VCM production, HCl is typically recycled via oxychlorination:

$$C_2H_4 + 2HCl + \frac{1}{2}O_2 \rightarrow C_2H_4Cl_2 + H_2O, \Delta H^{o}_{303K} = -566 \text{ kJ mol}^{-1}$$

For C_2H_6 chlorination, a similar HCl recovery loop can be implemented, as discussed in Section 4:

$$2HCl + \frac{1}{2}O_2 \rightarrow Cl_2 + H_2O, \Delta H^{o}_{303K} = -114 \text{ kJ mol}^{-1}$$

These thermodynamic data clearly indicate that C_2H_6 chlorination is strongly exothermic, releasing substantial heat that must be carefully managed in reactor design to ensure safe and efficient operation.

2.2 | Mechanistic Foundations of C_2H_6 Chlorination

The chlorination of C_2H_6 is predominantly governed by a radical chain mechanism. The initiation of •Cl can proceed via two principal pathways depending on the reaction conditions. Under non-catalytic conditions, •Cl is generated through thermal homolysis of Cl_2. This step has a high activation energy and thus becomes significant only at elevated temperatures (typically > 200 °C). In contrast, in the presence of a heterogeneous catalyst, a lower-energy pathway emerges. Catalytic surfaces, particularly those of rare-earth oxychlorides, can facilitate catalyst-assisted Cl_2 activation at moderate temperatures. This involves the heterolytic or homolytic cleavage of the Cl–Cl bond at surface sites, leading to the formation of adsorbed chlorine species that can readily desorb or participate in surface reactions.

Once generated, •Cl radicals rapidly abstract a hydrogen atom from C_2H_6 to form an ethyl radical (•C_2H_5) and HCl [38]. These •C_2H_5 then react with •Cl to produce C_2H_5Cl. Upon further chlorination, C_2H_5Cl is converted into dichloroethane through similar radical steps. The distribution of isomers, 1,1-$C_2H_4Cl_2$ and 1,2-$C_2H_4Cl_2$, is dictated by both kinetic and thermodynamic considerations. Specifically, the 1-chloroethyl radical (leading to 1,1-$C_2H_4Cl_2$) is more stable by approximately 15 kJ mol^{-1} than the 2-chloroethyl radical (leading to 1,2-$C_2H_4Cl_2$), resulting in a strong preference for 1,1-isomer formation under non-catalytic conditions [35]. This reaction network is depicted in Figure 2, which outlines the radical-mediated conversion of C_2H_6 to mono- and multi-chlorinated products via hydrogen abstraction and chlorine substitution.

Thermodynamic and kinetic analyses further support the dominance of •Cl-driven steps. Quantum chemical calculations reveal that hydrogen abstraction from C_2H_6 by •Cl has a low activation energy of 2.1 kJ mol^{-1} and is mildly exothermic (ΔH = –3.8 kJ mol^{-1}) [38]. In the case of C_2H_5Cl, hydrogen abstraction occurs without an energy barrier to form •$CHClCH_3$ (E_a = 0 kJ mol^{-1}), whereas the alternative pathway leading to •CH_2CH_2Cl is also accessible but requires a higher activation energy (E_a = 8.9 kJ mol^{-1}) [38]. These values explain why dichlorination becomes increasingly selective toward the 1,1-isomer under thermal conditions. Experimental observations agree with this theoretical prediction. In the absence of a catalyst, the product distribution of dichloroethane isomers consistently favors 1,1-$C_2H_4Cl_2$, with a typical molar ratio of 2:1 relative to the 1,2-isomer, invariant across a wide temperature range (250 °C–320 °C) and under various Cl_2 concentrations (Figure 3a,b) [39].

Interestingly, at temperatures exceeding 320 °C, new kinetic pathways become competitive under Cl_2-lean conditions (C_2H_6/Cl_2 molar ratio of 4:4). One such pathway involves the decomposition of the 2-chloroethyl radical, formed during the chlorination of C_2H_5Cl, to C_2H_4 and a •Cl, rather than undergoing further chlorination to produce 1,2-$C_2H_4Cl_2$ (Figure 3a) [39]. This pathway leads to the formation of C_2H_4, which becomes a dominant byproduct when the Cl_2 concentration is insufficient to sustain sequential chlorination. Thermal decomposition studies demonstrate that C_2H_5Cl remains stable even at 400 °C in the absence of Cl_2, confirming that C_2H_4 generation is not a consequence of direct thermal cleavage. Instead, C_2H_4 formation is mediated by chlorine radicals, which facilitate α-C–Cl bond scission through hydrogen abstraction (Figure 3c). This mechanistic bifurcation highlights the dual role of •Cl species, serving both as chlorinating agents and as drivers of dehydrochlorination, depending critically on their local concentration.

Moreover, the chlorination reactivity of C_2H_6 and its intermediates shows a clear declining trend with increasing chlorine substitution. The reactivity sequence under identical thermal conditions follows: $C_2H_6 > C_2H_5Cl > C_2H_4Cl_2 > C_2H_3Cl_3$. The primary factor responsible is a progressive decrease in the pre-exponential factor (A) in the Arrhenius expression [38]. This decline stems from increased molecular mass and moment of inertia upon chlorination, which lowers the effective frequency of reactive collisions. The chlorination of 1,2-$C_2H_4Cl_2$ is particularly slow, which reinforces the experimental observation that over-chlorination generally originates from 1,1-isomers rather than 1,2-isomers.

Despite the inherent exothermicity and favorable kinetics of C_2H_6 chlorination, the process lacks sufficient selectivity in the absence of catalytic control. The •Cl radical is highly reactive and non-discriminatory, such that over-chlorination and chain branching cannot be suppressed thermally. Therefore, while gas-phase radical chemistry provides an efficient activation strategy

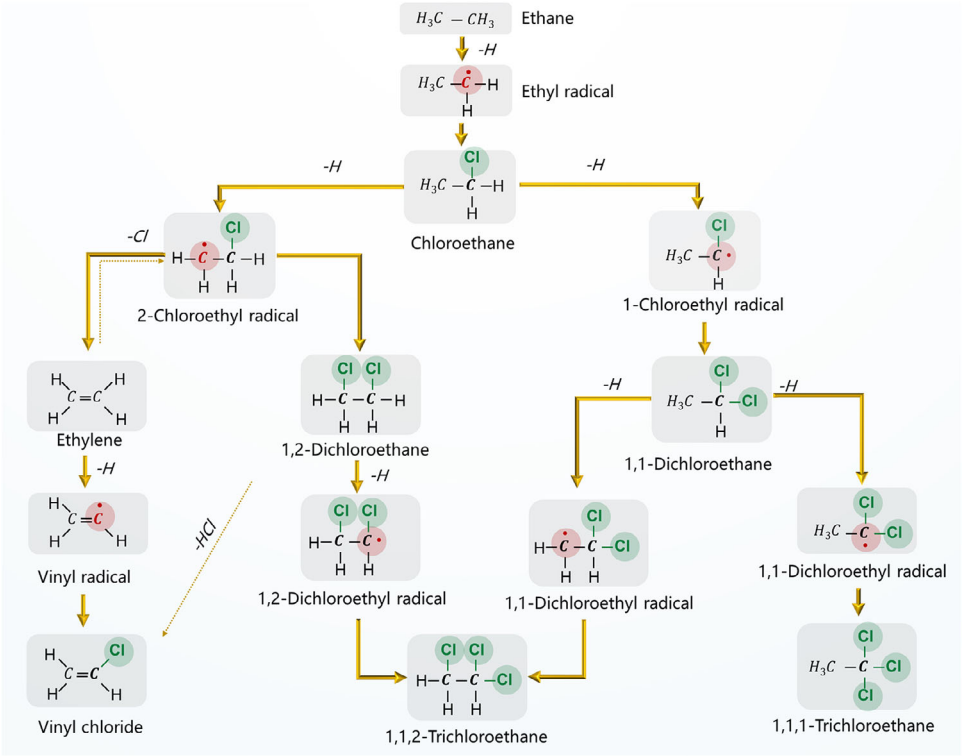

FIGURE 2 | Proposed reaction pathways for C_2H_6 chlorination via chlorine radical mechanisms.

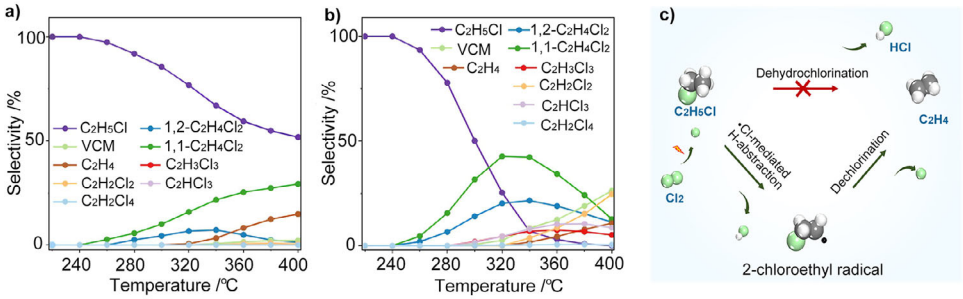

FIGURE 3 | Temperature-induced changes in radical reaction pathways during C_2H_6 chlorination under different feed compositions: (a) $C_2H_6/Cl_2/N_2$ = 4:4:92 (vol.%); (b) $C_2H_6/Cl_2/N_2$ = 4:8:88 (vol.%). (c) Proposed mechanism for •Cl-mediated dehydrochlorination of C_2H_5Cl to C_2H_4 via 2-chloroethyl radical intermediates. Reprinted from ref [39] with permission.

for inert C–H bonds, it also introduces selectivity challenges and complicates process scalability.

3 | Oxychloride-Based Catalysts for Selective C_2H_6 Chlorination

3.1 | Catalyst Design and Structural Evolution

Catalyst design for C_2H_6 chlorination plays a pivotal role not only in shifting product selectivity from undesired over-chlorinated species to target 1,2-$C_2H_4Cl_2$, but also in enabling long-term structural stability under aggressive Cl_2-rich conditions. Rare-earth oxychlorides, particularly LaOCl and EuOCl, have emerged as highly promising catalytic materials due to their ability to mediate Cl_2 activation and facilitate the transformation of intermediate species such as C_2H_5Cl into 1,2-$C_2H_4Cl_2$ (Figure 4) [40]. These catalysts exhibit high selectivity (> 80%) and sustained stability over extended operation periods under Cl_2-lean conditions (C_2H_6/Cl_2 molar ratio of 6:3).

Despite these advantages, structural evolution poses a significant challenge to the long-term selectivity of bulk oxychloride catalysts under industrially relevant conditions. Phase evolution studies have shown that under Cl_2-rich conditions (C_2H_6/Cl_2 molar ratio of 4:9), materials such as LaOCl progressively transform into $LaCl_3$ ($LaOCl + 2HCl \longrightarrow LaCl_3 + H_2O$, Figure 5a) [37]. As LaOCl constitutes the primary active phase responsible for the selective formation of 1,2-$C_2H_4Cl_2$, its structural degradation to $LaCl_3$ is strongly associated with a decline in 1,2-$C_2H_4Cl_2$ selectivity and a concomitant increase in over-chlorinated byproducts (Figure 5b). Interestingly, contrary to the postulate that the Lewis acidity of $LaCl_3$ might promote over-chlorination, a model catalyst study ($LaCl_3/Al_2O_3$) and theoretical calculations (Figure 5c)

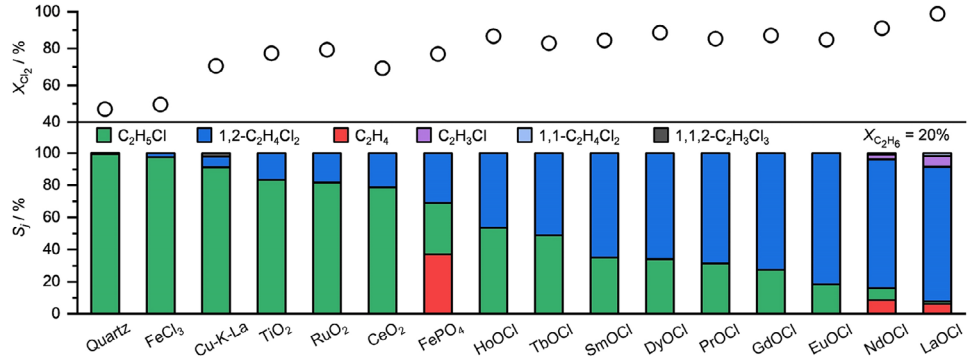

FIGURE 4 | Cl_2 conversion (top) and selectivity to product *j* (bottom) in C_2H_6 chlorination over the catalysts at approximately 20% C_2H_6 conversion. Reaction conditions: C_2H_6:Cl_2:Ar:He = 6:3:4.5:86.5, 287 °C–300 °C, 1 bar. Reprinted from ref [40]; Copyright 2021, John Wiley and Sons.

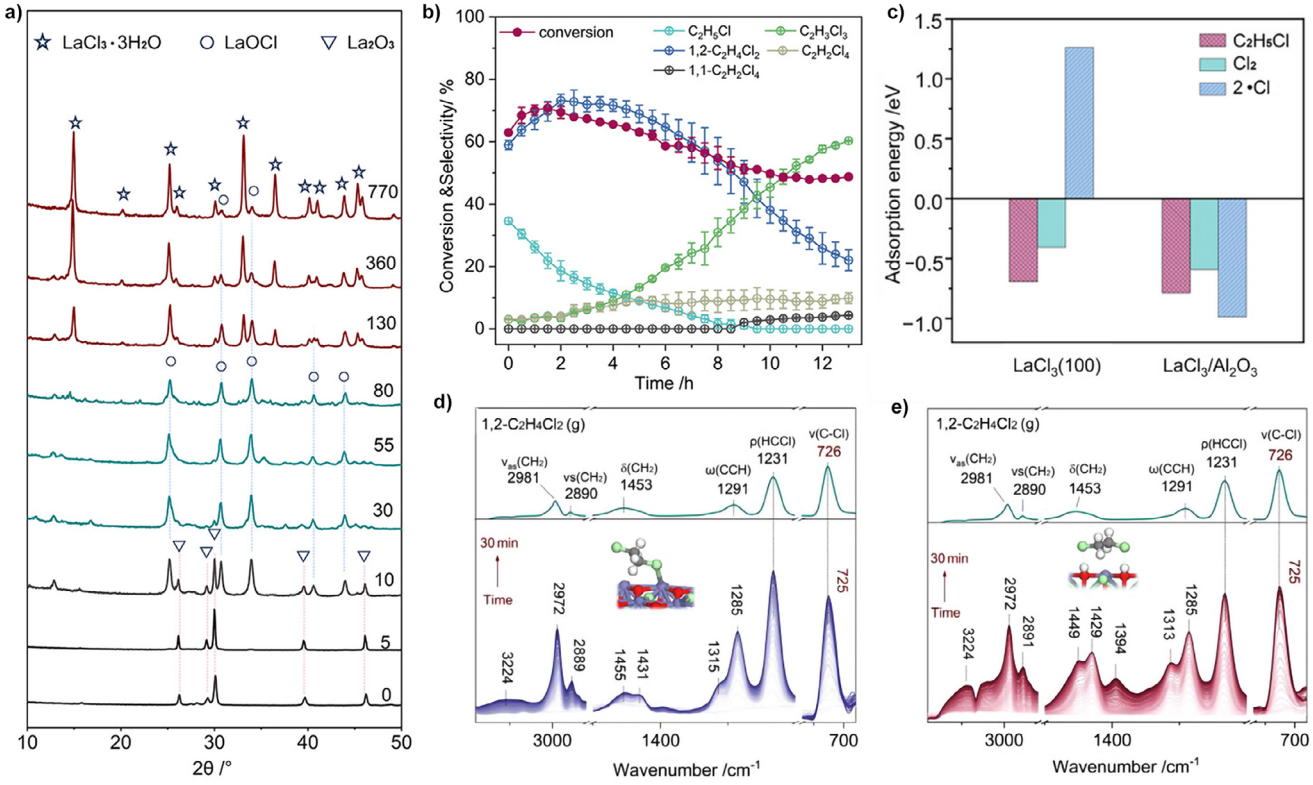

FIGURE 5 | (a) Time-resolved XRD patterns showing structural evolution of the La_2O_3 catalyst under reaction atmosphere. (b) Conversion and selectivity of C_2H_6 chlorination over the La_2O_3 catalyst. Reaction conditions: $C_2H_6/Cl_2/N_2$ = 4:9:87, 260 °C. (c) Adsorption energies of surface species on the sites of $LaCl_3/Al_2O_3$ and $LaCl_3$(100). In situ DRIFTS of 1,2-$C_2H_4Cl_2$ adsorption on La catalysts sampled at 55 min (d) and 770 min (e). Reprinted from ref [37] with permission.

demonstrate that aggregated $LaCl_3$ nanoparticles lack the ability to stabilize •Cl and consequently deactivate the surface sites, indicating that $LaCl_3$ formation itself is not the driving force behind 1,2-$C_2H_4Cl_2$ over-chlorination. Instead, it is primarily attributable to the accumulation of surface hydroxyl groups (–OH) during the phase transformation process. Specifically, surface –OH species enable bidentate adsorption of 1,2-$C_2H_4Cl_2$ through hydrogen bonding (Figure 5d,e), significantly increasing its adsorption strength (ΔE_{ad} = –1.35 eV, compared to –0.65 eV on hydroxyl-free surfaces). This enhanced adsorption facilitates the activation of C–Cl bonds and overcomes the energy barrier for subsequent chlorination. Therefore, the structural evolution of rare-earth oxychlorides under Cl_2-rich conditions, accompanied by hydroxyl accumulation, represents a critical bottleneck in maintaining long-term selectivity.

To address these limitations, recent studies have explored confinement strategies, with notable success achieved using Al_2O_3 as a structural stabilizer [41]. When La is introduced onto γ-Al_2O_3 via co-precipitation followed by calcination at 900 °C, the resulting $LaAl_2O_3$-like composite exhibits highly dispersed La species and strong La–O–Al interfacial bonding. The formation of La–O–Al linkages in catalysts is critical. These strong bonds electronically and structurally constrain the La centers, raising

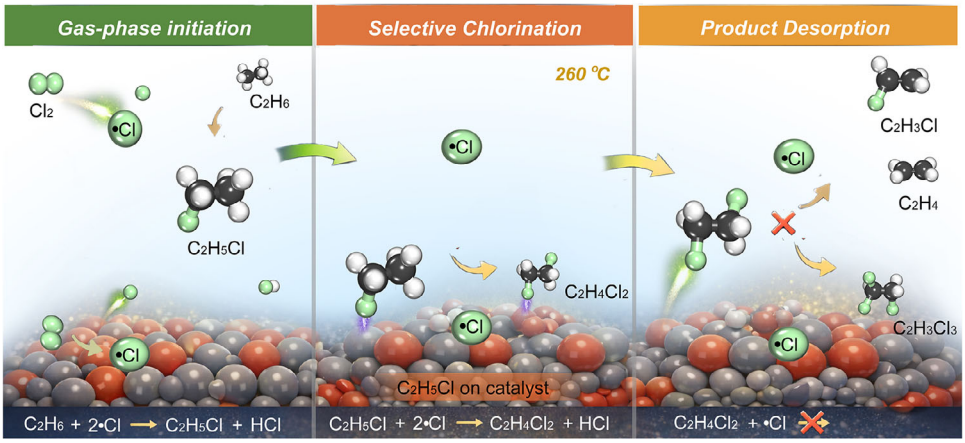

FIGURE 6 | Schematic illustration of the synergistic gas-phase •Cl and surface-catalyzed mechanism involved in C_2H_6 chlorination.

the energy barrier for their extraction and chlorination. This confinement maintains the local $LaOCl_x$ coordination environment, preventing the cascade toward $LaCl_3$ formation, thereby preserving its ability to stabilize •Cl and activate C_2H_5Cl selectively. The catalytic behavior of $LaAl_2O_3$ corroborates these structural findings. Under chlorination conditions of 260 °C and a C_2H_6/Cl_2 molar ratio of 4:9, $LaAl_2O_3$ maintains 61% C_2H_6 conversion with a stable 1,2-$C_2H_4Cl_2$ selectivity of 74% over 12 h. This stands in contrast to the rapid selectivity decline observed in bulk LaOCl systems.

The ability of rare-earth oxychlorides to mediate selective chlorination is considered analogous to that observed in CH_4 chlorination. For LaOCl-catalyzed oxidative chlorination of CH_4, a mechanism involving activation of surface chlorine by gas-phase O_2 to form OCl^- species was proposed, where the formal oxidation state of chlorine, rather than the La^{3+} center, cycles during the reaction [42]. This highlights the role of the oxychloride phase as a stable platform for chlorine redox chemistry. Consequently, the observed transformation of LaOCl to $LaCl_3$ under Cl_2-rich conditions during C_2H_6 chlorination likely represents a shift away from this catalytically active phase, underscoring the critical need for phase stabilization, as achieved in supported systems like $LaAl_2O_3$.

3.2 | Coupled Gas-Phase •Cl and Surface-Catalyzed Reactivity

The experimental and theoretical insights presented in previous sections rationalize the synergistic role of gas-phase radicals and the catalyst surface (Figure 6). The initiation of the reaction sequence—the activation of the strong C–H bonds in C_2H_6— proves challenging for most solid surfaces under mild conditions. In contrast, •Cl, whether generated thermally or via surface-assisted Cl_2 activation, abstracts hydrogen from C_2H_6 with a very low kinetic barrier. Consequently, the conversion of C_2H_6 to C_2H_5Cl is predominantly a gas-phase, •Cl-mediated process. This explains the frequently observed decoupling between catalyst activity: a catalyst may efficiently generate 1,2-$C_2H_4Cl_2$ at lower temperature, yet the conversion of C_2H_6 remains limited by the kinetics of radical attack in the gas phase.

The catalyst's pivotal role is unlocked upon the formation of the C_2H_5Cl intermediate. The introduction of a polar C–Cl bond enables a strong electronic interaction between C_2H_5Cl and the catalyst surface, typically through coordination of the Cl to Lewis-acidic metal sites (e.g., La^{3+} in LaOCl). This adsorption localizes and activates C_2H_5Cl for subsequent transformation. Importantly, the catalyst creates an alternative, lower-temperature route. By stabilizing reactive chlorine species and adsorbing C_2H_5Cl, it enables the second chlorination step to proceed efficiently at a lower temperature (~260 °C). This critical downshift in the operational temperature window for the selectivity-determining step is the key to suppressing undesirable gas-phase pathways. In the absence of such surface mediation, the sequential chlorination of 1,2-$C_2H_4Cl_2$ to $C_2H_3Cl_3$, along with competing dehydrochlorination to C_2H_2, are both propagated by •Cl and become significant at elevated temperatures (≥ 300 °C).

4 | Techno-Economic and Environmental Evaluation

The transition from traditional C_2H_4-based VCM production to emerging C_2H_6-based routes is increasingly justified by compelling techno-economic and environmental arguments. While the established business-as-usual (BAU) process—based on C_2H_4 chlorination and oxychlorination—has historically dominated the global VCM supply, its economic and environmental sustainability is being challenged by the volatility of petroleum markets and the need for carbon footprint mitigation. The evaluation of catalytic C_2H_6 chlorination technologies, therefore, involves a dual perspective: quantifying production costs and assessing lifecycle climate impacts under both current and projected energy systems.

From an environmental standpoint, the BAU route exhibits a global warming potential (GWP) of 1.87 kg CO_2-eq kg^{-1} VCM under the current 2020 energy scenario [23]. This impact arises primarily from C_2H_4 feedstock (46%), Cl_2 (20%), and O_2 (4%), with heating and cooling utilities accounting for 17% and 10%, respectively (Figure 7a). In comparison, the C_2H_6 route operated under realistic conditions—based on experimentally demonstrated catalytic performance (~90% selectivity at ~20% C_2H_6 conversion)—yields a moderately lower impact of 1.49 kg CO_2-eq

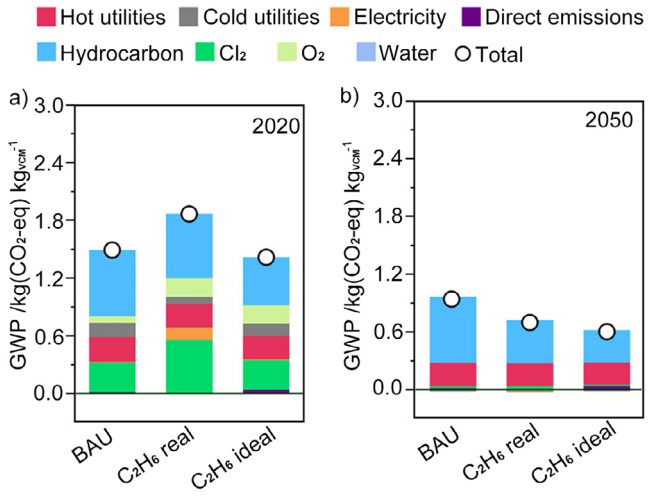

FIGURE 7 | Climate change impact breakdown of the two routes for VCM synthesis (BAU and C_2H_6 route, considering both the real and ideal scenarios) for both present (a) and future (b) temporal scenarios. The "hydrocarbon" contribution refers to C_2H_4 and C_2H_6 for the BAU and C_2H_6-based routes, respectively. Figure adapted from ref [23] with permission.

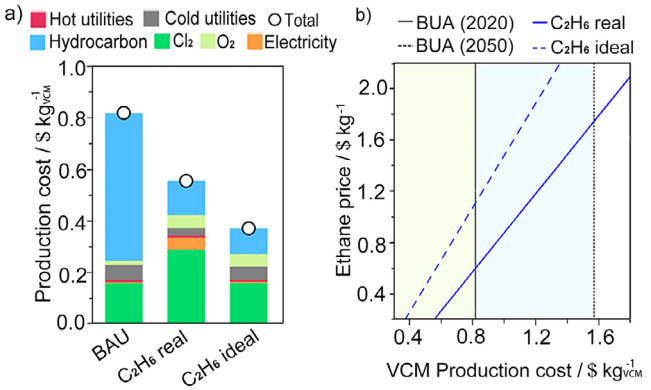

FIGURE 8 | (a) Economic results of the two routes for VCM synthesis (BAU and C_2H_6 routes). The "hydrocarbon" contribution refers to C_2H_4 and C_2H_6 for the BAU and C_2H_6-based route scenarios, respectively. (b) VCM production cost dependence on the C_2H_6 price of the two synthesis routes. The economic advantage of C_2H_6 chlorination technologies over the BAU is highlighted: green for the current scenario and blue for the prospective scenario. Figure adapted from ref [23] with permission.

kg^{-1} VCM, with raw materials (C_2H_6, Cl_2, O_2) contributing 36%, 30%, and 10%, respectively. Under ideal conditions (assuming 100% conversion and selectivity), the C_2H_6 route further reduces the GWP to 1.42 kg CO_2-eq kg^{-1} VCM, with raw materials contributing similarly but at lower absolute levels [23].

The environmental advantage of C_2H_6-based routes becomes more evident when prospective energy system decarbonization is considered [23]. Under the 2050 scenario aligned with the Paris Agreement (1.5 °C warming limit), the GWP of the BAU route falls to 0.95 kg CO_2-eq kg^{-1}, driven by improvements in the electricity mix and increased use of carbon capture technologies (Figure 7b). Still, the C_2H_6 route outperforms this benchmark, achieving a GWP of 0.70 kg CO_2-eq kg^{-1}. Under ideal conditions, its GWP is further reduced to 0.60 kg CO_2-eq kg^{-1}. This breakdown of environmental impacts highlights the central role of feedstock origin. In the 2050 scenario, C_2H_4 accounts for 73% of the BAU's GWP, whereas C_2H_6 contributes 72% to the C_2H_6 route (Figure 7b) [23].

Utility-related emissions are sensitive to energy source assumptions. The persistent large contribution of heating, 26% for BAU and 34% for the C_2H_6 real route in the 2050 scenario, stems from the continued fossil fuel use. This reveals a significant opportunity for further decarbonization. Electrifying process heating (e.g., cracking furnaces) using the projected carbon-neutral electricity mix of 2050 could reduce the 'heating' portion of the GWP to near zero. A preliminary estimate suggests this alone could lower the total GWP of the C_2H_6 real route by approximately an additional one-third, from 0.70 to about 0.46 kg CO_2-eq kg^{-1} VCM [23]. Thus, coupling catalyst innovation with the electrification of thermal units is paramount for achieving deep decarbonization of VCM production.

Chlorine's marginal impact (2%–4%) reflects its relatively modest energy footprint when derived from modern chloralkali processes powered by renewable electricity. Sensitivity analyses further demonstrate the robustness of the C_2H_6 routes to feedstock volatility. While the BAU cost escalates sharply with C_2H_4 price (Figure 8a), the C_2H_6-based processes remain economically viable across a broad range of C_2H_6 price points. For instance, the C_2H_6 route remains cheaper than BAU even with a threefold increase in C_2H_6 price (Figure 8b) [23].

Environmental competitiveness, however, depends on achieving sufficiently high product selectivity. At a fixed conversion (~20%), increasing selectivity to 89% would render the C_2H_6 routes environmentally preferable to BAU even in today's energy context [23]. This is because most environmental burdens associated with utilities are driven by separation processes needed to remove byproducts. Therefore, integrated improvements in both catalyst development and reactor design (e.g. Cl_2 stage-feeding strategies) are crucial to close the remaining 14%–22% selectivity gap and unlock the full environmental benefits. It is important to note that this selectivity threshold of ~89% for the C_2H_6 route to outperform the BAU environmentally is calculated under the assumption of fixed C_2H_6 conversion. In practice, a key catalytic challenge is the trade-off between conversion and selectivity; achieving higher conversion while maintaining high selectivity is essential for overall process efficiency. Future, more detailed techno-economic analyses that explicitly couple conversion and selectivity would offer more precise guidance for process optimization.

Importantly, the techno-economic viability of C_2H_6-based VCM production also depends on the efficiency with which the chlorine loop is closed. Two distinct HCl recycling strategies can be considered: direct C_2H_6 oxychlorination and a two-step process combining Deacon oxidation with separate C_2H_6 chlorination. In the direct route, HCl and O_2 are co-fed with C_2H_6, ideally following reactions such as $C_2H_6 + 2HCl + ½O_2 \rightarrow C_2H_4Cl_2 + H_2O$, but in practice O_2 simultaneously promotes deep oxidation ($C_2H_6 + O_2 \rightarrow CO_x + H_2O$). Even state-of-the-art oxychlorination catalysts typically achieve < 50% selectivity to VCM [43], translating into higher separation costs and inferior carbon efficiency. Notably, direct C_2H_6 oxychlorination generally

requires elevated temperatures above ~450 °C to activate the C_2H_6. Under such conditions, the simultaneous presence of HCl, O_2, and H_2O creates an exceptionally aggressive environment that accelerates catalyst deactivation. In contrast, the two-step route decouples oxidation and chlorination. HCl is first oxidized via the Deacon reaction ($4HCl + O_2 \rightarrow 2Cl_2 + 2H_2O$), after which C_2H_6 chlorination proceeds in an O_2-free environment, followed by highly selective 1,2-$C_2H_4Cl_2$ cracking to VCM (> 99%). This separation enables selectivity > 80% to 1,2-$C_2H_4Cl_2$ and allows independent optimization of each reactor. Although involving more unit operations, the two-step strategy aligns with established VCM plant architectures and relies on mature technologies, making it the more reliable pathway for closing the chlorine loop.

5 | Outlook

The catalytic chlorination of C_2H_6 has emerged as a compelling alternative to the conventional C_2H_4-based route for VCM production, driven by resource availability and decarbonization imperatives. Despite recent progress, however, the field remains at an early stage of development. Translation from laboratory-scale demonstrations to industrially viable technologies is hindered by interconnected challenges spanning •Cl-mediated reaction pathways and catalyst durability. Addressing these challenges requires a shift from empirical optimization toward a more mechanistically grounded research framework.

A key limitation of the current study is the insufficient molecular-level understanding of •Cl-mediated chlorination on the catalyst surface. Compared to the extensive study on CH_4 chlorination, systematic studies of C_2H_6 chlorination remain scarce, particularly with respect to the electronic structure and kinetics of surface-associated •Cl species. Consequently, the activation and transformation pathways of Cl_2 and chlorinated intermediates on catalyst surfaces remain poorly understood. This gap hampers rational interpretation of experimental selectivity trends, such as the near-complete suppression of 1,1-$C_2H_4Cl_2$ formation on catalyst surfaces despite its thermodynamic accessibility in the gas phase. Bridging this gap will require the combined application of surface-sensitive characterization and theory-driven kinetic modeling, with explicit consideration of radical–surface interactions and their temporal evolution under reaction conditions.

From a catalyst design standpoint, current research has focused predominantly on rare-earth oxychloride systems, which exhibit high selectivity and resistance to deep chlorination. While these materials establish an important performance benchmark, their reliance on rare-earth elements raises legitimate concerns regarding cost, supply robustness, and long-term scalability. In this context, insights from earlier studies on CH_4 chlorination offer valuable catalyst design principles. Foundational studies on solid acids, including zeolites and sulfated metal oxides, showed that electrophilic chlorination pathways can be promoted at the expense of uncontrolled radical chain reactions, enabling selective mono-chlorination [44–46]. Translating these design principles to C_2H_6 chlorination, while mitigating catalyst sintering and structural degradation, represents a promising route toward expanding the catalyst landscape beyond rare-earth-based materials.

Equally critical, yet comparatively underexplored, is the role of reactor engineering in governing selectivity and stability. C_2H_6 chlorination is intrinsically dominated by highly exothermic radical reactions, rendering precise control over temperature and reactant concentration profiles indispensable. The widespread reliance on fixed-bed reactors with uniform feed composition limits the ability to regulate axial Cl_2/C_2H_6 ratios and suppress secondary chlorination. Future progress will likely depend on reactor concepts that enable spatial and temporal control of chlorine availability, such as staged Cl_2 feeding, dynamic residence time modulation, and the incorporation of quenching or dilution zones.

Given the geographic abundance of natural gas—particularly in North America and the Middle East, which together account for over 48 million tons of C_2H_6 annually—C_2H_6 offers a regionally secure and economically attractive alternative to oil-derived C_2H_4. On the environmental front, utilizing C_2H_6 aligns with long-term decarbonization strategies, especially when renewable-sourced Cl_2 and electrified heating become mainstream. In this sense, the adoption of C_2H_6 chlorination technologies supports the dual objectives of reducing reliance on petroleum-derived feedstocks and meeting carbon mitigation targets without the need for policy enforcement. In conclusion, emerging C_2H_6-based routes for VCM production present a compelling case for both environmental sustainability and economic resilience. Realizing this potential will require sustained, interdisciplinary efforts and a commitment to closing the laboratory-to-market gap.

Acknowledgments

This work is financially supported by the National Natural Science Foundation of China (Grant No. 22478385), the NSFC Centre for Single-Atom-Catalysis (Grant No. 22388102), the DICP.CAS-Cardiff Joint Research Units (121421ZYLH20230008), and the CAS Project for Young Scientists in Basic Research (YSBR-022).

Conflicts of Interest

The authors declare no conflict of interest.

Data Availability Statement

The data that support the findings of this study are available from the corresponding author upon reasonable request.

References

1. K. Mulder and M. Knot, "PVC Plastic: A History of Systems Development and Entrenchment," *Technology in Society* 23 (2001): 265–286, https://doi.org/10.1016/S0160-791X(01)00013-6.

2. P. Johnston, N. Carthey, and G. J. Hutchings, "Discovery, Development, and Commercialization of Gold Catalysts for Acetylene Hydrochlorination," *Journal of the American Chemical Society* 137 (2015): 14548–14557, https://doi.org/10.1021/jacs.5b07752.

3. R. Geyer, J. R. Jambeck, and K. L. Law, "Production, Use, and Fate of All Plastics Ever Made," *Science Advances* 3 (2017): e1700782.

4. Y. Bao, X. Zheng, J. Cao, et al., "Free Radicals Induced Ultra-rapid Synthesis of N-Doped Carbon Sphere Catalyst With Boosted Pyrrolic N Active Sites for Efficient Acetylene Hydrochlorination," *Nano Research* 16 (2023): 6178–6186, https://doi.org/10.1007/s12274-022-5237-y.

5. A. Schade, M. Melzer, S. Zimmermann, T. Schwarz, K. Stoewe, and H. Kuhn, "Plastic Waste Recycling—A Chemical Recycling Perspective," *ACS Sustainable Chemistry & Engineering* 12 (2024): 12270–12288, https://doi.org/10.1021/acssuschemeng.4c02551.

6. G. J. Hutchings, "Vapor Phase Hydrochlorination of Acetylene: Correlation of Catalytic Activity of Supported Metal Chloride Catalysts," *Journal of Catalysis* 96 (1985): 292–295, https://doi.org/10.1016/0021-9517(85)90383-5.

7. G. Malta, S. A. Kondrat, S. J. Freakley, et al., "Identification of Single-Site Gold Catalysis in Acetylene Hydrochlorination," *Science* 355 (2017): 1399–1403, https://doi.org/10.1126/science.aal3439.

8. S. K. Kaiser, I. Surin, A. Amorós-Perez, et al., "Design of Carbon Supports for Metal-Catalyzed Acetylene Hydrochlorination," *Nature Communications* 12 (2021): 4016, https://doi.org/10.1038/s41467-021-24330-2.

9. H. Ma, Y. Wang, Y. Qi, K. R. Rout, and D. Chen, "Critical Review of Catalysis for Ethylene Oxychlorination," *ACS Catalysis* 10 (2020): 9299–9319, https://doi.org/10.1021/acscatal.0c01698.

10. C. Li, R. Liu, Z. Zhang, et al., "Engineering Charge Polarized Au Sites for Low-Temperature Acetylene Hydrochlorination," *Angewandte Chemie International Edition* 64 (2025): e202501370.

11. Z. Chen, Y. Chen, S. Chao, et al., "Single-Atom Au I –N 3 Site for Acetylene Hydrochlorination Reaction," *ACS Catalysis* 10 (2020): 1865–1870, https://doi.org/10.1021/acscatal.9b05212.

12. J. Li, J. Fan, S. Ali, et al., "The Origin of the Extraordinary Stability of Mercury Catalysts on the Carbon Support: The Synergy Effects Between Oxygen Groups and Defects Revealed From a Combined Experimental and DFT Study," *Chinese Journal of Catalysis* 40 (2019): 141–146, https://doi.org/10.1016/S1872-2067(19)63271-7.

13. Z. Chen, S. Wang, J. Zhao, and R. Lin, "Advances in Single-Atom-Catalyzed Acetylene Hydrochlorination," *ACS Catalysis* 14 (2024): 965–980, https://doi.org/10.1021/acscatal.3c04495.

14. H. Ma, G. Ma, Y. Qi, et al., "Nitrogen-Doped Carbon-Assisted One-Pot Tandem Reaction for Vinyl Chloride Production via Ethylene Oxychlorination," *Angewandte Chemie International Edition* 59 (2020): 22080–22085, https://doi.org/10.1002/anie.202006729.

15. G. Zichittella, N. Aellen, V. Paunovic, A. P. Amrute, and J. Pérez-Ramírez, "Olefins From Natural Gas by Oxychlorination," *Angewandte Chemie International Edition* 56 (2017): 13670–13674, https://doi.org/10.1002/anie.201706624.

16. N. B. Muddada, U. Olsbye, L. Caccialupi, et al., "Influence of Additives in Defining the Active Phase of the Ethylene Oxychlorination Catalyst," *Physical Chemistry Chemical Physics* 12 (2010): 5605, https://doi.org/10.1039/b926502n.

17. C. Lamberti, C. Prestipino, F. Bonino, et al., "The Chemistry of the Oxychlorination Catalyst: An In Situ, Time-Resolved XANES Study," *Angewandte Chemie International Edition* 41 (2002): 2341–2344, https://doi.org/10.1002/1521-3773(20020703)41:13%3c2341::AID-ANIE2341%3e3.0.CO;2-P.

18. Z. Vajglová, N. Kumar, K. Eränen, M. Peurla, D. Y. Murzin, and T. Salmi, "Ethene Oxychlorination Over CuCl2/γ-Al2O3 Catalyst in Micro- and Millistructured Reactors," *Journal of Catalysis* 364 (2018): 334–344, https://doi.org/10.1016/j.jcat.2018.05.019.

19. J. A. Incavo, "A Detailed Quantitative Study of 1,2-Dichloroethane Cracking to Vinyl Chloride by a Gas Chromatographic Pyrolysis Device," *Industrial & Engineering Chemistry Research* 35 (1996): 931–937, https://doi.org/10.1021/ie9505017.

20. R. Schirmeister, J. Kahsnitz, and M. Träger, "Influence of EDC Cracking Severity on the Marginal Costs of Vinyl Chloride Production," *Industrial & Engineering Chemistry Research* 48 (2009): 2801–2809, https://doi.org/10.1021/ie8006903.

21. S. M. Al-Zahrani, A. M. Aljodai, and K. M. Wagialla, "Modelling and Simulation of 1,2-Dichloroethane Production by Ethylene Oxychlorination in Fluidized-Bed Reactor," *Chemical Engineering Science* 56 (2001): 621–626, https://doi.org/10.1016/S0009-2509(00)00268-2.

22. K. E. Howlett, "Pyrolysis of 1.2 Dichlorethane," *Nature* 165 (1950): 860, https://doi.org/10.1038/165860a0.

23. J. D. Medrano-García, V. Giulimondi, A. Ceruti, G. Zichittella, J. Pérez-Ramírez, and G. Guillén-Gosálbez, "Economic and Environmental Competitiveness of Ethane-Based Technologies for Vinyl Chloride Synthesis," *ACS Sustainable Chemistry & Engineering* 11 (2023): 13062–13069, https://doi.org/10.1021/acssuschemeng.3c03006.

24. F. Benyahia, "The VCM Process Economics: Global and Raw Material Impacts," in *Proceedings of the 1st Annual Gas Processing Symposium*, eds. H. E. Alfadala, G.V. R. Reklaitis, and M. M. El-Halwagi (Elsevier, 2009), 415–422.

25. J. Zhong, Y. Xu, and Z. Liu, "Heterogeneous Non-Mercury Catalysts for Acetylene Hydrochlorination: Progress, Challenges, and Opportunities," *Green Chemistry* 20 (2018): 2412–2427, https://doi.org/10.1039/C8GC00768C.

26. G. Czakó and J. M. Bowman, "Dynamics of the Reaction of Methane with Chlorine Atom on an Accurate Potential Energy Surface," *Science* 334 (2011): 343–346, https://doi.org/10.1126/science.1208514.

27. M. Bilke, P. Losch, O. Vozniuk, A. Bodach, and F. Schuth, "Methane to Chloromethane by Mechanochemical Activation: A Selective Radical Pathway," *Journal of the American Chemical Society* 141 (2019): 11212–11218, https://doi.org/10.1021/jacs.9b04413.

28. Y. Wang, R. Hu, Y. Liu, et al., "The Enhanced Catalytic Performance of Mg2+-Doped CuCr2O4 Catalyst in Ethane Oxychlorination," *Journal of Catalysis* 373 (2019): 228–239, https://doi.org/10.1016/j.jcat.2019.03.040.

29. D. Shi, R. Hu, Q. Zhou, and C. Li, "Effect of Cr-Doping on CuCl2-KCl-CeO2/γ-Al2O3 Catalysts for Ethane Oxychlorination," *Applied Catalysis A: General* 506 (2015): 91–99, https://doi.org/10.1016/j.apcata.2015.08.037.

30. C. Li, G. Zhou, L. Wang, S. Dong, J. Li, and T. Cheng, "Effect of Ceria on the MgO-γ-Al2O3 Supported CeO2/CuCl2/KCl Catalysts for Ethane Oxychlorination," *Applied Catalysis A: General* 400 (2011): 104–110, https://doi.org/10.1016/j.apcata.2011.04.017.

31. Z. Li, G. Zhou, C. Li, and T. Cheng, "Effect of Pr on Copper-Based Catalysts for Ethane Oxychlorination," *Catalysis Communications* 40 (2013): 42–46, https://doi.org/10.1016/j.catcom.2013.05.020.

32. A. Gvakharia, E. A. Kort, A. Brandt, et al., "Methane, Black Carbon, and Ethane Emissions From Natural Gas Flares in the Bakken Shale, North Dakota," *Environmental Science & Technology* 51 (2017): 5317–5325, https://doi.org/10.1021/acs.est.6b05183.

33. D. Helmig, S. Rossabi, J. Hueber, et al., "Reversal of Global Atmospheric Ethane and Propane Trends Largely Due to US Oil and Natural Gas Production," *Nature Geoscience* 9 (2016): 490–495, https://doi.org/10.1038/ngeo2721.

34. G. Zichittella, A. Ceruti, G. Guillén-Gosálbez, and J. Pérez-Ramírez, "Catalyst: A Step Forward for PVC Manufacture From Natural Gas," *Chemistry* 8 (2022): 883–885, https://doi.org/10.1016/j.chempr.2022.02.012.

35. M. Wang and D. Ma, "Reaction: Direct Chlorination of Ethane to Dichloroethane," *Chemistry* 8 (2022): 886–887.

36. R. Zheng, Z. Liu, and Z. Xie, "Reaction: Process Changes of PVC Manufacture Driven by Ethane Chlorination," *Chemistry* 8 (2022): 888–889.

37. Y. Li, H. Qi, Z. Zhu, et al., "Dynamic Active Site Evolution in Lanthanum-Based Catalysts Dictates Ethane Chlorination Pathways," *Angewandte Chemie International Edition* 64 (2025): e202505846, https://doi.org/10.1002/anie.202505846.

38. I. M. Dahl, E. M. Myhrvold, U. Olsbye, F. Rohr, O. A. Rokstad, and O. Swang, "On the Gas-Phase Chlorination of Ethane," *Industrial & Engineering Chemistry Research* 40 (2001): 2226–2235, https://doi.org/10.1021/ie000850n.

39. Z. Zhu, Y. Li, X. Wu, J. Xu, X. Sun, and Q. Liu, "Unraveling the Kinetics and Mechanism of Ethane Chlorination in the Gas Phase," *Molecules (Basel, Switzerland)* 30 (2025): 1756, https://doi.org/10.3390/molecules30081756.

40. G. Zichittella and J. Pérez-Ramírez, "Ethane-Based Catalytic Process for Vinyl Chloride Manufacture," *Angewandte Chemie International Edition* 60 (2021): 24089–24095, https://doi.org/10.1002/anie.202105851.

41. Y. Li, Z. Zhu, X. Wu, L. Ma, X. Sun, and Q. Liu, "Metastable LaOClx Phase Stabilization as an Effective Strategy for Controllable Chlorination of Ethane Into 1,2-Dichloroethane," *Molecules (Basel, Switzerland)* 30 (2025): 1746, https://doi.org/10.3390/molecules30081746.

42. S. G. Podkolzin, E. E. Stangland, M. E. Jones, E. Peringer, and J. A. Lercher, "Methyl Chloride Production From Methane Over Lanthanum-Based Catalysts," *Journal of the American Chemical Society* 129 (2007): 2569–2576, https://doi.org/10.1021/ja066913w.

43. L. Yang, R. Hu, H. Li, Y. Jia, Q. Zhou, and H. Wang, "The Effect of Interaction Between La 2 AlCoO 6 and CuCl 2 on Ethane Oxychlorination," *Journal of Industrial and Engineering Chemistry* 56 (2017): 120–128, https://doi.org/10.1016/j.jiec.2017.07.004.

44. S. Kwon, H.-J. Chae, and K. Na, "Control of Methane Chlorination With Molecular Chlorine Gas Using Zeolite Catalysts: Effects of Si/Al Ratio and Framework Type," *Catalysis Today* 352 (2020): 111–117, https://doi.org/10.1016/j.cattod.2020.01.014.

45. H. Joo, D. Kim, K. S. Lim, Y. N. Choi, and K. Na, "Selective Methane Chlorination to Methyl Chloride by Zeolite Y-Based Catalysts," *Solid State Sciences* 77 (2018): 74–80, https://doi.org/10.1016/j.solidstatesciences.2018.01.010.

46. Y. Kim, J. Kim, H. W. Kim, et al., "Sulfated Tin Oxide as Highly Selective Catalyst for the Chlorination of Methane to Methyl Chloride," *ACS Catalysis* 9 (2019): 9398–9410, https://doi.org/10.1021/acscatal.9b02645.